Photometric Stereo-based Defect Detection for Lithium Battery Top Covers

Huayong Li[a], Weijin Xie[a], Wei Pan*[b]
[a]School of Mechanical Engineering, Dongguan University of Technology, DongGuan, GuangDong, China,523808; [b]OPT Machine Vision Tech Co., Ltd., DongGuan, GuangDong, China, 523850
* Corresponding author: vpan@foxmail.com

ABSTRACT

Detecting surface defects on lithium battery top covers is critical for ensuring their performance, reliability, and longevity. Photometric stereo (PS) methods, known for their ability to capture detailed surface topography with high precision and speed, have been widely applied in industrial defect detection. However, these methods often face challenges in dynamic scenes with varying lighting conditions and in detecting subtle defects such as shallow scratches. To address these limitations, we propose an enhanced approach that combines the advantages of photometric stereo with a line-scan camera and weighted least squares filtering. This novel combination improves the contrast of surface defects, particularly in fine or shallow scratches, by enhancing the surface detail and minimizing noise. Experimental results demonstrate the effectiveness of this method, showing significant improvements in the detection accuracy and sensitivity to fine defects on the battery end surfaces.

Keywords: Photometric stereo, defect detection, image enhancement, online detection

1. INTRODUCTION

Cylindrical lithium batteries are widely employed in industries such as new energy vehicles and mobile electronics, owing to their exceptional performance. With the rapid advancement of society and the economy, consumer demand for higher battery quality has surged. However, during the production process, these batteries are susceptible to surface defects such as scratches and pits caused by collisions, friction, and external forces[1]. These defects not only undermine product quality and company reputation but also affect consumer satisfaction and usage reliability. Therefore, detecting surface defects on battery top covers is critically important. Surface defects refer to deviations between the surfaces of defective and standard products, with scratches and pits being the most common types. Traditionally, human visual inspection has been the primary approach for identifying these defects. While still widely used in the manufacturing industry, visual inspection suffers from significant limitations, including low sampling rates, poor accuracy, inefficiency, high labor demands, and vulnerability to human error.

To overcome these shortcomings, automated surface defect detection has become a critical focus of research. With advancements in Charge-Coupled Device (CCD) technology, image processing, and computer vision, machine vision inspection has emerged as a leading approach for automated surface defect detection[2]. Machine vision is widely applied in various industrial automation fields, offering significant advantages over human inspection, such as higher resolution, objective evaluation, automation, and fatigue-free operation. Surface defect detection based on machine vision can be broadly categorized into two-dimensional (2D) and three-dimensional (3D) approaches. 2D methods, renowned for their simplicity and ease of implementation, utilize image processing techniques to identify defects[3]. However, they are often ineffective for bright or dark surfaces and are prone to interference from text, dirt, and other factors due to the lack of depth information. Moreover, the reflectivity of metal surfaces makes it difficult to achieve accurate detection in bright and dark areas, complicating the distinction between interference and actual defects. As a result, traditional 2D methods are inadequate for detecting defects on battery end surfaces. On the other hand, 3D methods, such as structured light[4] and fringe projection[5], offer more precise defect detection by utilizing depth information but tend to be costly and data-intensive.

The Photometric Stereo (PS) method, first introduced by Professor R.J. Woodham in 1980[6], extracts three-dimensional models from two-dimensional texture data, making it highly effective for detecting subtle surface changes. PS has been

Seventh International Conference on Image Processing and Machine Vision
(IPMV 2025), edited by Hui Zhang, Proc. of SPIE Vol. 13636, 136360E
 · 0277-786X · doi: 10.1117/12.3062071

widely applied in industries such as steel[7], carbon fiber[8], and leather[9] due to its ability to capture fine surface details. The method involves capturing images of an object under varying lighting directions and solving a system of reflection equations, based on Lambertian reflectance, to determine surface normals and curvature[10]. This approach enables 3D object reconstruction, facilitating defect detection using 3D data.

However, achieving optimal 3D reconstruction typically requires numerous light sources, which increases both image acquisition and computational costs. To address this, curvature data derived from PS can be directly utilized for defect detection through image processing, as explored in this paper[11]. Despite its effectiveness, traditional PS is constrained to static objects, limiting its application in industrial scenarios. Moreover, detecting subtle defects remains challenging, necessitating further methodological optimizations.

Recent advancements in PS have sought to overcome these limitations. For example, Xiaokang Ren employed a four-light-source PS approach for label defect detection[12]. Wang L utilized red, green, and blue light sources to capture grayscale images from a single color image, though interference between RGB channels remains an issue[13]. Haoyue Liu and colleagues developed an online defect detection system for gearbox covers using a combined image registration method[14]. Shun Wang introduced a symmetric dual-light-source PS (TLPS) algorithm, enhancing efficiency and accuracy in surface defect detection[15]. Meanwhile, Hamish Dow utilized angular and directional illumination to generate 3D meshes and measure peeling volume with the aid of three neural networks[16], significantly improving data interpretation and reducing imaging time.

This paper introduces an enhanced photometric stereo method using a line-scan camera, which retains the simplicity of traditional PS techniques while enabling high-precision, high-speed online defect detection for battery end surfaces. Our approach incorporates both hardware and algorithmic improvements to facilitate effective online detection of surface defects. The feasibility of the method has been validated through experimental results. Section 2 outlines the principles of the enhanced PS method, Section 3 presents the experimental design and results, and Section 4 discusses potential future research directions.

2. THEORY AND METHOD

2.1. Hardware Setup

Traditional photometric stereo systems typically capture images under static workpiece conditions, which can provide accurate results in controlled environments. However, real-world engineering applications increasingly require real-time monitoring of moving objects to improve automation and production efficiency. To address this need, we propose the use of a line-scan camera in combination with time-division strobe settings. The high-speed imaging capability of the line-scan camera, along with time-division multiplexing, allows for the sequential activation of directional lighting in a continuous cycle, facilitating the imaging process. A motion platform generates a line signal, which is processed by a frequency divider to produce four signals that independently control the activation of four directional light sources while simultaneously triggering the camera’s image capture. To achieve uniform illumination, we employed a four-section spherical integrating light source, enhancing the synthesis of photometric stereo.

Traditional spherical integrating light sources typically feature a circular aperture at the top of the dome for image capture. However, this design can introduce shadows that degrade image quality. Shadows obscure fine details on the object's surface and interfere with subsequent data processing and analysis, thereby reducing detection accuracy and reliability. To address this issue, we modified the traditional spherical integrator by replacing the circular aperture with a narrow slit, effectively reducing shadow artifacts. This modification significantly enhanced the clarity of the captured images, making subtle defects more visible.

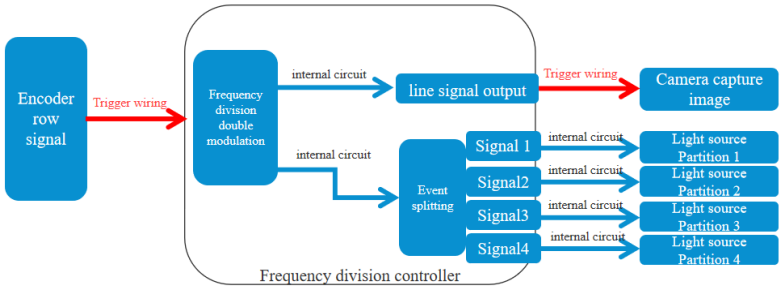

Figure 1. Flow chart of signal transmission

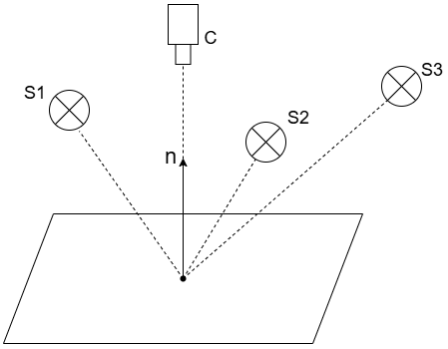

Figure 2. Photometric stereo schematic diagram

2.2. Improved Photometric Stereo Method

The intensity of diffuse reflection light is calculated according to the Lambertian ideal diffuse reflection model using formula (1):

$$I = \rho LN \tag{1}$$

Where I is the brightness of a single pixel in the image of the object being measured; ρ is the surface reflectance of the object; L is the unit direction vector of the light source; and N is the unit normal vector of the object's surface.

Photometric stereo is a technique that uses at least three images captured from different lighting directions to reconstruct the surface of an object. This method leverages varying lighting angles to provide rich information about light and shadow variations, allowing the system to effectively extract surface features and details, thereby achieving more accurate three-dimensional reconstruction. To further improve imaging accuracy, we adopted a strategy of increasing the number of light sources, adding additional constraints to enhance reconstruction precision. This approach not only enables more accurate estimation of surface gradient information but also significantly improves image quality, resulting in a more realistic and refined final output. However, increasing the number of lighting directions also means that the number of images to process will increase, thereby prolonging processing time. Therefore, after careful consideration, we employed a four-light-source photometric stereo approach. The resulting system of equations is as follows:

$$\begin{cases} \mathrm{I}_1 = \rho\left(\mathrm{L}_\mathrm{x}^1\mathrm{N}_\mathrm{x} + \mathrm{L}_\mathrm{y}^1\mathrm{N}_\mathrm{y} + \mathrm{L}_\mathrm{z}^1\mathrm{N}_\mathrm{z}\right) \\ \mathrm{I}_2 = \rho\left(\mathrm{L}_\mathrm{x}^2\mathrm{N}_\mathrm{x} + \mathrm{L}_\mathrm{y}^2\mathrm{N}_\mathrm{y} + \mathrm{L}_\mathrm{z}^2\mathrm{N}_\mathrm{z}\right) \\ \mathrm{I}_3 = \rho\left(\mathrm{L}_\mathrm{x}^3\mathrm{N}_\mathrm{x} + \mathrm{L}_\mathrm{y}^3\mathrm{N}_\mathrm{y} + \mathrm{L}_\mathrm{z}^3\mathrm{N}_\mathrm{z}\right) \\ \mathrm{I}_4 = \rho\left(\mathrm{L}_\mathrm{x}^4\mathrm{N}_\mathrm{x} + \mathrm{L}_\mathrm{y}^4\mathrm{N}_\mathrm{y} + \mathrm{L}_\mathrm{z}^4\mathrm{N}_\mathrm{z}\right) \end{cases} \tag{2}$$

The resulting system of equations can be expressed in matrix form as follows:

$$\begin{bmatrix} I_1 \\ I_2 \\ I_3 \\ I_4 \end{bmatrix} = \rho \begin{bmatrix} L_x^1 & L_y^1 & L_z^1 \\ L_x^2 & L_y^2 & L_z^2 \\ L_x^3 & L_y^3 & L_z^3 \\ L_x^4 & L_y^4 & L_z^4 \end{bmatrix} \begin{bmatrix} N_x \\ N_y \\ N_z \end{bmatrix} \tag{3}$$

By applying the least squares method, we can solve for the unit normal vector N of the object：

$$N = \frac{(L^T L)^{-1}(L^T L)}{\rho} \tag{4}$$

Due to curvature being a measure of the unevenness of a surface, we can assume the measured surface is described by Z=f(x,y). The surface gradients (p,q) can be calculated as follows (5):

$$p = \frac{\partial f}{\partial x}, q = \frac{\partial f}{\partial y} \tag{5}$$

Based on (6), we can easily obtain the curvature map, which is used for defect detection in image processing methods.

$$\begin{aligned} A &= \left(1 + \frac{\partial f(r,c)^2}{\partial r}\right)\frac{\partial^2 f(r,c)}{\partial c^2} \\ B &= \frac{\partial f(r,e)\,\partial f(r,c)}{\partial r}\left(\frac{\partial^2 f(r,c)}{\partial r\,\partial c} + \frac{\partial^2 f(r,c)}{\partial c\,\partial r}\right) \\ C &= \left(1 + \frac{\partial f(r,c)^2}{\partial c}\right)\frac{\partial^2 f(r,c)}{\partial r^2} \\ D &= \left(1 + \frac{\partial f(r,c)^2}{\partial r} + \frac{\partial f(r,c)^2}{\partial c}\right)^{\frac{3}{2}} \\ H &= \frac{A-B+C}{D} \end{aligned} \tag{6}$$

Gaussian curvature is calculated as follows.

$$K = \frac{\frac{\partial f(r,c)^2}{\partial r\,\partial r} * \frac{\partial f(r,c)^2}{\partial c\,\partial c} - \frac{\partial f(r,c)^2}{\partial r\,\partial c} * \frac{\partial f(r,c)^2}{\partial c\,\partial r}}{\left(1 + \frac{\partial f(r,c)^2}{\partial r} + \frac{\partial f(r,c)^2}{\partial c}\right)^2} \tag{7}$$

By applying contrast stretching and adjusting the transformation coefficients, we can enhance the grayscale differences on the curvature map, thereby highlighting defect areas:

$$I = (Z - ZMin)/(ZMax - ZMin) * (GrayMax - GrayMin) + GrayMin \tag{8}$$

In this context, I denotes the brightness of a pixel in the image, while ρ represents the surface reflectance. Z Min and ZMax represent the minimum and maximum depth values, respectively. GrayMin corresponds to the minimum depth associated with the image's minimum gray value, and GrayMax corresponds to the maximum depth associated with the image's maximum gray value. L is the unit direction vector of the light source, and N is the unit normal vector of the object's surface.

In industrial battery defect detection, there is a strong demand for high processing efficiency. To improve system performance, we employed CUDA technology for accelerated processing. Specifically, we transfer image data to the GPU to fully leverage its powerful parallel computing capabilities. This approach enables efficient parallel computation on the device side, significantly increasing processing speed. Once the computation is complete, the results are transferred back to the host, which not only enhances overall operational efficiency but also provides timely feedback for subsequent data processing.

In the resulting curvature images, surface texture interference and subtle scratches make certain details less distinct. To address this issue, we applied the least squares filtering method to smooth the images. The weighted least squares filter is an effective edge-preserving technique designed to smooth the image while retaining significant edges[17]. During processing, this filter smooths regions with smaller gradients while preserving the clarity of important edge features. This smoothing process enhances the visual quality of the image and provides a stronger foundation for subsequent analysis and processing. The loss function f(u) can be expressed as follows:

$$\sum_p \left((u_p - g_p)^2 + \lambda \left(a_{x,p}(g) \left(\frac{\partial u}{\partial x}\right)_p^2 + a_{y,p}(g) \left(\frac{\partial u}{\partial y}\right)_p^2 \right) \right) \tag{9}$$

Where the original graph is g and the filtered result to be solved is u。α_x，$\alpha_y$are the weight matrices of the gradients in the x and y directions, respectively。By adjusting the parameters, the weighted least squares filter can smooth the texture of the workpiece on the image while retaining defects such as scratches, so as to improve the success rate of defect detection.

2.3 Defect detection

After synthesizing the photometric stereo images, it is crucial to extract defect information for effective defect detection. The first step involves selecting a region of interest (ROI), which helps reduce the computational load and removes interference from other areas. Next, we preprocess the image, which generally includes filtering and sampling. Downsampling involves reducing the original image size to filter out noise, minimizing information redundancy while still retaining key details. Upsampling, on the other hand, adds new elements between existing pixels using suitable interpolation methods to enlarge the image, enhance resolution, and increase detail. Filtering techniques aim to suppress noise while preserving important image characteristics, often employing low-pass filters such as mean filtering, median filtering, and Gaussian filtering to effectively reduce noise interference.

Once preprocessing is complete, we perform a differential operation to obtain a difference image. By comparing the original and preprocessed images, this differential processing effectively emphasizes the differences, making scratches and other anomalies more noticeable. When detecting surface defects on the top cover of cylindrical lithium batteries, the difference image shows significant improvement. This method clearly highlights defect features while significantly reducing background noise, thereby enhancing the accuracy and reliability of defect detection.

Thresholding is then applied to binarize the image, enabling layered analysis based on different threshold ranges. After binarization, defect areas appear in high-contrast black and white, which clarifies the shapes, locations, and sizes of defects such as scratches and dents, providing a reliable foundation for subsequent automatic detection and classification. Morphological operations, such as erosion and dilation, can further refine the boundaries of target objects. For example, erosion smooths and tightens the edges. Finally, defects are accurately extracted based on their grayscale and regional features.

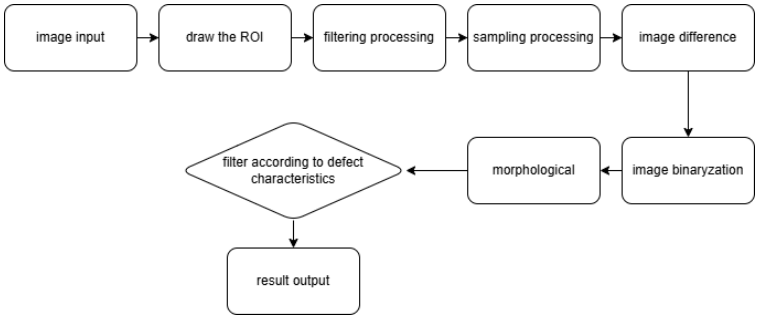

Figure 3. Flow chart of defect detection

3. EXPERIMENTS AND RESULTS

A photometric stereo platform was developed using a partitioned spherical integrator as the light source for image acquisition. The light source consists of a four-part spherical integrator to ensure uniform illumination within each section, while a line-scan camera is employed for image capture. The system is powered by an industrial computer equipped with a 12th Gen Intel® Core™ i5-12500 processor, running at 3.00 GHz, and an Nvidia GeForce RTX 3060 GPU. The GPU is equipped with 3,584 CUDA cores, 65,536 bytes of global memory, and 49,152 bytes of shared memory. The GPU block sizes range from 16 to 32.

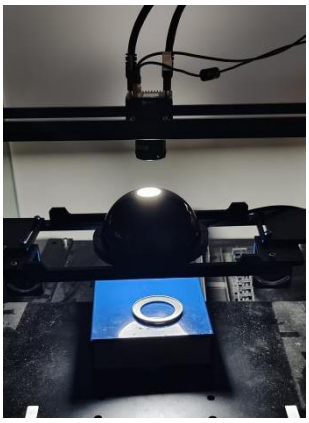

Figure 4. Photometric stereo platform

After setting up the image acquisition platform, we first calibrate the light source using a ring light to determine the light direction vectors. The position of the light source remains fixed while capturing four images of the battery cover surface based on the calibrated directions.

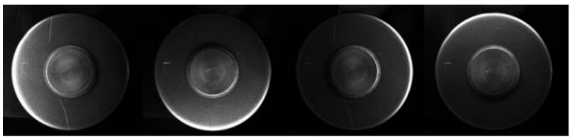

Figure 5. Captured image of the battery surface

The images are transferred to the device for parallel processing using CUDA, which enhances computational efficiency and reduces processing time, ultimately generating reflectance and curvature images. The reflectance image is used to detect foreign objects and contaminants on the surface, while the curvature image helps identify scratches, wrinkles, and other defects.

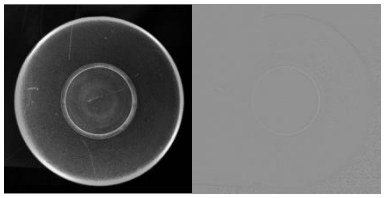

Figure 6.Images of albedo and mean curvature

Next, we stretch the average curvature image to enhance the contrast of subtle defects and apply weighted least squares filtering to minimize texture interference. The resultant images are evaluated using metrics such as image clarity, information entropy, variance, PSNR, and SSIM, and compared with the results from Method 12 in the literature. The findings show that all five metrics outperform Method 12, demonstrating that our approach enhances defect contrast while preserving the original image structure, thereby improving defect detection accuracy.

Table 1 Image quality evaluation metrics

	Sharpness	Entropy	Variance	PSNR	SSIM
Paper 12 Methods	16.90861336	4.160162157	41.02653361	10.84012553	0.512343764
Method of this paper	77.05879915	4.698335101	168.8762457	12.36584077	0.526821911

While the Intel Thread Building Blocks (TBB) library can be used for parallel computation on the CPU, its performance is considerably lower compared to GPU-based parallel processing. We evaluated the performance of photometric stereo and processing speeds across different image sizes. For CPU-based computations, TBB was combined with parallel acceleration, while CUDA was used for GPU parallel processing. The experimental results show that GPU-based parallel acceleration significantly enhances computational efficiency.

After synthesizing the photometric stereo images, a scratch detection algorithm is applied to identify defects. First, a region of interest is selected to reduce computational load. Next, a differential operation is performed, and the resulting difference image is binarized. Defect detection is then carried out based on shape and grayscale features.

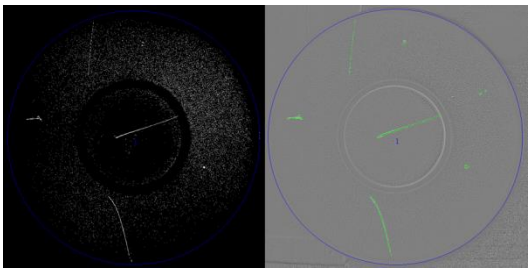

Figure 7. Binarized image and detection result

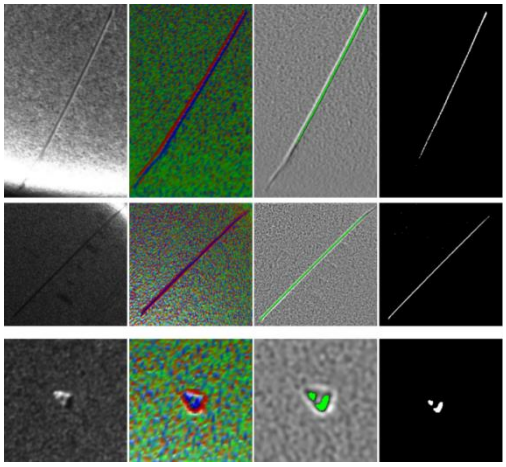

Figure 8. Detail diagram of defect extraction

The results demonstrate that photometric stereo imaging achieves high precision in detecting defects on battery covers, meeting the stringent requirements of industrial production. To validate the detection accuracy, we collected 100 images of aluminum alloy surfaces with known defects, applied photometric stereo synthesis, and recorded the success rate.

Table 2 Statistics of defect detection

	Total defects	Number of missed detection	detection rate
scratch	376	16	95.38%
Pit	336	12	96.43%

4. CONCLUSION AND FUTURE WORK

This paper proposed an improved photometric stereo method for detecting surface defects on battery covers. By utilizing a line-scan camera and applying weighted least squares filtering, the method enhances the contrast and clarity of subtle defects, leading to higher detection accuracy. Experimental results show that this design significantly improves imaging quality by effectively minimizing shadow artifacts, thereby enhancing image clarity and detail presentation. Future work will focus on refining the algorithm to detect defects on non-Lambertian surfaces and further improving real-time processing efficiency.

REFERENCES

[1] Guo Shaotao, YUAN Weiqi. Cylindrical lithium-ion battery end pit defect detection method research [J]. Journal of instruments and meters,230-239.(2022).

[2] Yang Zeqing, ZHANG Mingxuan, Chen Yingshu, et al. Surface defect detection method based on machine vision research progress [J]. Modern manufacturing engineering,143-156(2023).

[3] Sharifzadeh M, Amirfattahi R, Sadri S, et al. Detection of steel defect using the image processing algorithms[C]//The International Conference on Electrical Engineering. Military Technical College, 2008, 6(6th International Conference on Electrical Engineering ICEENG ,1-7(2008)

[4] Geng J. Structured-light 3D surface imaging: a tutorial[J]. Advances in optics and photonics,3(2): 128-160(2011).

[5] Liu Z, Jin Y, Wu J, et al. The online measurement of appearance quality for stainless steel plates based on grating projections[J]. Insight-Non-Destructive Testing and Condition Monitoring,60(5): 257-263(2018).

[6] Woodham R J. Photometric method for determining surface orientation from multiple images[J].Optical Engineering, 19(1):139-144(1980).

[7] Kang D, Jang Y J, Won S. Development of an inspection system for planar steel surface using multispectral photometric stereo[J]. Optical Engineering,52(3): 039701-039701(2013).

[8] Palfinger W, Thumfart S, Eitzinger C. Photometric stereo on carbon fiber surfaces[C]//35th Workshop of the Austrian Association for Pattern Recognition(2011).

[9] Chen Z, Deng J, Zhu Q, et al. A systematic review of machine-vision-based leather surface defect inspection[J]. Electronics, 11(15): 2383(2022).

[10] Woodham R J. Gradient and curvature from the photometric-stereo method, including local confidence estimation[J]. JOSA A, 11(11): 3050-3068(1994).

[11] Zhang H, Niu Y, Zhang H. Small target detection based on difference accumulation and Gaussian curvature under complex conditions[J]. Infrared Physics & Technology, 87: 55-64(2017).

[12] Ren X, Wang W, Ren J, et al. Research and application of label defect detection method based on machine vision[C]//Journal of Physics: Conference Series. IOP Publishing, 1453(1): 012084(2020).

[13] Wang L, Xu K, Zhou P. Online detection technique of 3D defects for steel strips based on photometric stereo[C]//2016 Eighth International Conference on Measuring Technology and Mechatronics Automation (ICMTMA). IEEE, 428-432(2016).

[14] Liu H, Wu X, Yan N, et al. An improved photometric stereo method for the online defect detection of gearbox covers[C]//2022 8th International Conference on Nanomanufacturing & 4th AET Symposium on ACSM and Digital Manufacturing (Nanoman-AETS). IEEE,1-6(2022).

[15] Wang S, Xu K, Li B, et al. Online micro defects detection for ductile cast iron pipes based on twin light photometric stereo[J]. Case Studies in Construction Materials,19: e02561(2023).

[16] Dow H, Perry M, Pennada S, et al. 3D reconstruction and measurement of concrete spalling using near-field Photometric stereo and YOLOv8[J]. Automation in Construction,166: 105633(2024).

[17] Farbman Z, Fattal R, Lischinski D, et al. Edge-preserving decompositions for multi-scale tone and detail manipulation[J]. ACM transactions on graphics (TOG), 27(3): 1-10(2008)